Systematic Comparisons between Broken Symmetry and Symmetry-Adapted Approaches to Transition States by Chemical Indices: A Case Study of the Diels−Alder Reactions†

Hiroshi Isobe,*,‡ Yu Takano,‡ Yasutaka Kitagawa,‡ Takashi Kawakami,‡ Syusuke Yamanaka,‡ Kizashi Yamaguchi,‡ and K. N. Houk§

Department of Chemistry, Graduate School of Science, Osaka University, Osaka, 560-0043, Japan, and Department of Chemistry and Biochemistry, University of California at Los Angeles, Los Angeles, California 90095-1565

Received: May 7, 2002; In Final Form: November 13, 2002

Systematic comparisons between broken symmetry (BS) and symmetry-adapted (SA) approaches to transition states were carried out using chemical indices, which are defined using the occupation numbers of natural orbitals (NOs) by both BS and SA methods. For the former, unrestricted Hartree−Fock, UMP2, UQCISD(T), and UCCSD(T), together with hybrid density functional theory (DFT) methods such as UB2LYP and UB3LYP, were employed, while CASSCF, UNO CASCI, UNO CASCI MP2 (≡ CASMP2(CI)), and MRMP2 were used for the latter approach. To begin with, we examined the functional behaviors of chemical indices during the C−C bond dissociation process of ethylene or the least motion association reaction of triplet methylenes. The bonding characteristics revealed by the chemical indices are largely dependent on the computational methods. Next, the energy difference between concerted and nonconcerted transition structures of the Diels−Alder reaction of butadiene and ethylene was calculated by both BS and SA methods. The origin of excellent energetics by the hybrid DFT methods for this reaction was revealed in terms of the chemical indices. These indices are also useful to understand the nature of the chemical bonds at TSs and the role of unstable intermediates in stepwise mechanisms. Furthermore, the ability of phenyl groups to stabilize nonsynchronous TS for the Diels−Alder and the Cope rearrangement reactions was examined by the NO analyses of the BS hybrid DFT solutions. The difference of the chemical indices for substituted systems provides useful information for the theoretical consideration of the reaction mechanism and stereospecificity of pericyclic reactions. Finally, implications of the computational results are discussed in relation to appropriate selection of effective hybrid DFT methods for large systems with moderate radical characters, for which the SA computations are difficult.

Introduction

Energy differences between concerted (CTSs) and nonconcerted (NTSs) transition structures in pericyclic reactions have received continuous attention, since stereospecificity is a central issue in developing effective syntheses of chemical substances.[1−7] However, quantitative calculations of such energies are not easy because they are so sensitive to electron correlation effects. Both symmetry-adapted (SA) and broken-symmetry (BS) ab initio computational methods have been employed for the purpose by many research groups. For example, with the SA approach, limited CI, CASSCF, CASPT2, and related multireference (MR) theories[8−10] have been applied to estimate activation barrier heights for the TSs in the Diels−Alder, the Cope rearrangement, and other pericyclic reactions. The BS approaches such as unrestricted Hartree−Fock (UHF), UMP2, UCCSD(T),[11−13] and spin-polarized density functional (UDFT) theories[14−17] have also been utilized for the computations of the energy differences between the transition (CTS and NTS) structures. Although the SA approaches are desirable, their applicability is limited to small molecules. The BS methods are applicable to large systems, but they often provide apparently different pictures of chemical bonds. The common criteria between the SA and the BS approaches are, therefore, necessary for deeper understanding of the nature of the chemical bonds at TSs.

Recently, one of the hybrid DFT methods,[18−21] B3LYP, provided excellent energetics for CTS and NTS. The nonconcerted paths determined by the method often exhibit diradical character because spin-polarized B3LYP (UB3LYP) solution becomes the most stable at such nonsynchronous geometry. However, it has been found that the diradical character for NTS is quenched significantly or diminished if pure DFT such as BLYP is used.[22] To clarify the origin of such a difference, the natural orbital (NO) analysis of UHF, UB2LYP, UB3LYP, and UBLYP solutions is crucial since the SA CASCI and CASSCF results can be used as the standard references for comparison. To extract common footings between the BS and the SA methods, we here define and express spin density index (Q), unpaired electron density (U),[22,24,25] effective bond order (b), information entropy (I),[26−29] and diradical character (y)[23] in terms of the occupation number (n) of NO by both methods. This in turn enables us to select effective BS DFT methods, which reproduce the SA CAS results.

To understand the behaviors of five chemical indices (Q, U, b, I, and y) by the BS methods, their functional dependencies on the strength of π and σ covalent bonds of ethylene are first examined during its dissociation process or the least motion

† Extended Hartree−Fock (EHF) Theory of Chemical Reactions. Part VII.

* To whom correspondence should be addressed. Tel: +81-6-6850-5405. Fax: +81-6-6850-5550. E-mail: isobe@chem.sci.osaka-u.ac.jp.

‡ Osaka University.

§ University of California at Los Angeles.

10.1021/jp021125o CCC: $25.00
Published on Web 01/04/2003

association reaction of two triplet methylenes. The rotational energy barriers around the C−C bond are also examined to interpret the interrelationship between the chemical indices and the nonstereospecificity. These indices are also used to elucidate the different characteristics among the BS methods. For example, it will be shown that UHF and UBLYP overestimate and underestimate the diradical character, respectively, while the hybrid DFT methods reproduce the CAS results, indicating the applicability for larger systems with diradical characters.

To elucidate the nature of the chemical bonds at TSs, five chemical indices are calculated for both concerted and stepwise mechanisms of the Diels−Alder reaction between butadiene and ethylene by using NOs and their *n* values of both SA and BS wave functions. Stabilization of NTS by the introduction of phenyl groups is also examined through the NO analyses of UHF and hybrid UDFT solutions. The analysis shows that 18 π NO 18 electron, CAS {18, 18}, are necessary for the Diels−Alder reactions involving two phenyl groups. Therefore, CASSCF {18, 18} and CASPT2 {18, 18}[10] are desirable for quantitative SA treatments of the reactions, but these are impossible. On the other hand, BS hybrid DFT calculations of them followed by the NO analysis combined with chemical indices are handy and practical as an alternative to CASPT2 at the present stage of computational chemistry. The same computations are also feasible to explain the diradical stabilization by phenyl groups for the Cope rearrangement reactions. Implications of the present SA and BS computational results are discussed in relation to applicability and reliability of hybrid DFT methods toward TSs of pericyclic reactions with and without diradical characters.

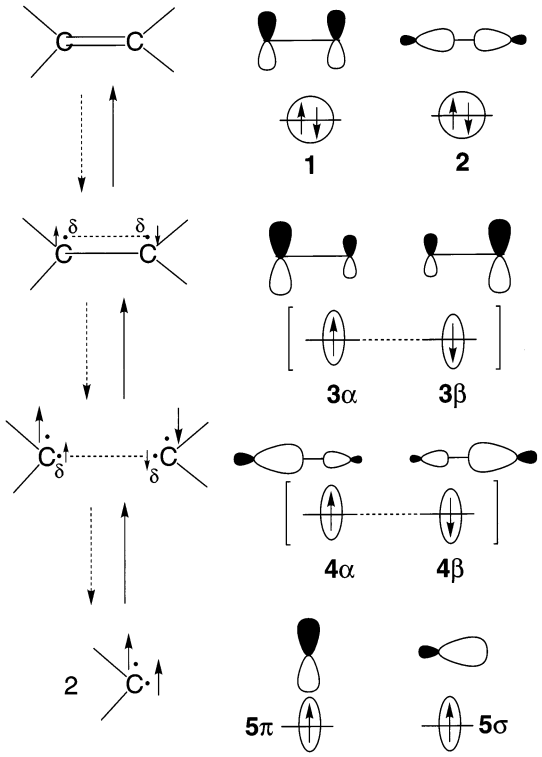

Figure 1. Closed shell (**1** and **2**) and open shell (**3** and **4**) orbital configurations of ethylene at the equilibrium and C−C elongated geometries.

Definitions of Chemical Indices

An important problem in theoretical organic chemistry is to understand the nature of the chemical bonds at TSs and unstable reaction intermediates. The theoretical description is now feasible by several molecular orbital (MO) type models such as hybrid UDFT methods. As an example, let us first consider the putative C−C dissociation reaction of ethylene by the least motion path to form two triplet methylenes (CH_2) in order to clarify chemical characteristics by the generalized MO (GMO) method.[23] The bonding and antibonding C−C π and σ bonds are given by the SA MO as[23,30−33]

$$\phi^{\kappa} = \frac{1}{\sqrt{2}}(\chi_a^{\kappa} + \chi_b^{\kappa}),\ \phi^{\kappa^*} = \frac{1}{\sqrt{2}}(\chi_a^{\kappa} - \chi_b^{\kappa}) \tag{1}$$

where χ_c^{κ} denotes the orthogonalized atomic orbital at site c (= a and b) and $\kappa = \pi$ or σ. The closed shell π and σ bonds are formed by the occupation of each bonding MO by the α and β spin electrons at the equilibrium geometry ($R_{C-C} = 1.34$ Å) of ethylene as shown in **1** and **2** of Figure 1. However, these MOs become spin-polarized even at the low-spin (LS) singlet state of the C−C elongated geometry

$$\psi_{\pm}^{\kappa} = \cos\theta_{\kappa}\phi^{\kappa} \pm \sin\theta_{\kappa}\phi^{\kappa^*} \tag{2}$$

where θ_{κ} is the orbital mixing parameter determined by GMO methods such as UHF and UDFT. The closed shell π orbital in **1** splits into the α and β spin π MOs in **3**, which are localized to various extents on the left and right carbon atoms, respectively, as in the case of the generalized VB (GVB) orbitals,[23] and finally become equivalent to the atomic p orbitals (AOs) as shown in Figure 1. Because the bonding and antibonding MOs have different spatial symmetries, the split MOs are of BS. This entails the singlet $\pi\pi$ diradical configuration given by **3** in Figure 1. The closed shell σ orbital in **2** also splits into the α and β spin MOs (**4**) at the more C−C elongated geometry, which has the tetraradical character. Finally, two triplet methylenes (**5**) are generated at the dissociation limit ($R = \infty$).

To express variations of the π and σ bonds in the C−C dissociation or association process, several theoretical indices are introduced. The orbital overlap between the α and the β spin−orbitals is defined as a measure of orbital splitting[23] by

$$T^{\kappa} = \langle\psi_+^{\kappa}|\psi_-^{\kappa}\rangle = \cos 2\theta_{\kappa} \tag{3}$$

where T^{κ} is 1.0 for the closed shell MO ($\theta_{\kappa} \equiv 0$, and α and β orbitals are identical) like **1** and **2**, and $0 \le T^{\kappa} < 1.0$ for the open shell systems ($\theta_{\kappa} \neq 0$) like **3** and **4**. In contrast to GMO, T^{κ} by GVB is always smaller than 1.0 because of inclusion of the dynamical correlation. The occupation numbers of the bonding and antibonding MOs in eq 1 are given by T^{κ} as

$$n^{\kappa} = 1 + T^{\kappa},\ n^{\kappa^*} = 1 - T^{\kappa} \tag{4}$$

those are 2 and 0 for closed shell and 1 and 1 for pure diradical. The effective bond order for the κ bond is expressed by

$$b^{\kappa} = \frac{n^{\kappa} - n^{\kappa^*}}{2} = T^{\kappa} \tag{5}$$

where $b^{\kappa} = 1$ for **1** and **2** because $n^{\kappa} = 2$, $n^{\kappa^*} = 0$, and $T^{\kappa} = 1$, while $b^{\kappa} < 1$ for **3** and **4** since $n^{\kappa} < 2$, $n^{\kappa^*} > 0$, and $T^{\kappa} < 1$. The orbital overlap (T^{κ}) and effective bond order (b^{κ}) are closely related in the GMO theory, where the SA MO splits into two AOs through the BS MOs during the covalent bond dissociation.[23]

Because the α and β spins enter the different MOs in eq 2, the spin densities appear even in the singlet diradical state described under the BS approximation as

$$^{LS}Q^{\kappa} = (\psi_{+}^{\kappa})^2 - (\psi_{-}^{\kappa})^2 = \sqrt{1-(T^{\kappa})^2}\{(\chi_a^{\kappa})^2 - (\chi_b^{\kappa})^2\} \quad (6a)$$

$$^{LS}Q_a^{\kappa} = -^{LS}Q_b^{\kappa} = \sqrt{1-(T^{\kappa})^2} \quad (6b)$$

This means that the α and β spin densities are populated on the left and right carbon atoms, respectively.

The electronic structure of molecules with the electron pair splitting can be described by both SA and BS methods. It seems desirable to invent a general method of drawing information about the splitting of electron pairs from the exact and approximate wave functions. The deviation of the diagonal element of the density matrix for any wave function from that of the single Slater determinant is given by Löwdin,[24] Takatsuka et al.,[25] and Staroverov et al.[22]

$$U(r) = 2\Gamma_1(r) - (\Gamma_1(r))^2 \quad (7a)$$

where Γ_1 is the first-order density matrix[22−25] and $U(r)$ denotes the density function or unpaired electron density.[22,24,25] The density function can be expanded diagonally in terms of the NOs and their occupation numbers by using eqs 1−4 as

$$^{LS}U^{\kappa} = n^{\kappa}(2-n^{\kappa})(\phi^{\kappa})^2 + n^{\kappa}(2-n^{\kappa})(\phi^{\kappa^*})^2 \quad (7b)$$

$$= \{1-(T^{\kappa})^2\}\{(\chi_a^{\kappa})^2 + (\chi_b^{\kappa})^2\} \quad (7c)$$

$$^{LS}U_a^{\kappa} = {}^{LS}U_b^{\kappa} = 1-(T^{\kappa})^2 = \Delta^{LS}\langle S^2\rangle \quad (7d)$$

The unpaired electron densities are positive in sign, and their magnitude is nothing but the deviation of total spin angular momentum from the exact singlet value $^{LS}\langle S^2\rangle = 0$ for the BS solution. The ^{LS}U values are chemically responsible for electron pair splitting in diradical species.[22]

Classical and quantum information entropies are now well-defined in several different fields to extract information. In chemistry, information entropy (I)[26−29] is employed to express the characteristic of chemical bonds. The Jaynes information entropy is defined by the occupation numbers of NOs for diradical configuration to express electron correlation

$$I_D^{\kappa} = -n^{\kappa}\ln n^{\kappa} = -(1+T^{\kappa})\ln(1+T^{\kappa}) \quad (8a)$$

The I^{κ} value is reduced to $I_c^{\kappa} = -2\ln 2$ for the closed shell configuration ($T^{\kappa} = 1$), which has the maximum negative entropy, while the I^{κ} value is zero for the pure diradical with $T^{\kappa} = 0$. The normalized information entropy I_n^{κ} for κ bond is defined by

$$I_n^{\kappa} = \frac{I_c^{\kappa} - I_D^{\kappa}}{I_c^{\kappa}} = \frac{2\ln 2 - (1+T^{\kappa})\ln(1+T^{\kappa})}{2\ln 2} \quad (8b)$$

The I_n^{κ} value increases with the decrease of T^{κ} in this definition and is parallel to the decrease of the effective bond order $\Delta b = 1-b = 1-T^{\kappa}$. The I_n^{κ} and Δb values are responsible for loss of bond formation or bond breaking. Recently, Smith and co-workers have succeeded in making a connection between unpaired electron density and information entropy.[29b]

CASCI and CASSCF methods[8−10] are well-accepted approaches to open shell species. It is desirable to clarify mutual relations between the CI and the BS methods. The diradical character (y) is defined by the weight of doubly excited configuration (W_D) involved in the singlet-projected BS solution for comparison with CASCI and CASSCF[23,34,35] as

$$y^{\kappa} = 2W_D = 1 - \frac{2T^{\kappa}}{1+(T^{\kappa})^2} \quad (9a)$$

$$= \frac{\{(n^{\kappa})^2 - 4n^{\kappa} + 4\}}{\{(n^{\kappa})^2 - 2n^{\kappa} + 2\}} \quad (9b)$$

The y^{κ} values are 100% for complete diradical ($T^{\kappa} = 0$) and 0% for closed shell configurations ($T^{\kappa} = 1$) **1** and **2** in Figure 1. All of the chemical indices are related to each other through the occupation numbers of NOs calculated by both SA and BS solutions. These indices can be used as common criteria for chemical bonds described by both of the solutions. This is not at all trivial since the former SA method becomes hardly applicable to large systems such as enzymes. Utility of such NO analysis to remove apparent differences of several wave functions has been demonstrated in the case of the 1,3-dipolar species.[23]

Functional Behaviors of Chemical Indices

Computational Procedure. BS calculations, HF, QCISD(T), CCSD(T), BLYP, B2LYP, and B3LYP were performed with Gaussian 94,[36] while SA calculations, CASSCF, MRMP2, UNO CASCI, and UNO CASCI MP2 (≡ CASMP2 (CI)) calculations were carried out with GAMESS.[37] The 6-31G* basis set[38] was used throughout the calculations.

In the hybrid DFT calculations,[18−21] exchange correlation functionals are defined by

$$E^{XC} = C_1E_X^{HF} + C_2E_X^{Slater} + C_3\Delta E_X^{Becke88} + C_4E_C^{VWN} + C_5\Delta E_C^{LYP} \quad (10)$$

where the first and second terms indicate HF and Slater exchange functionals, respectively. The third and fourth terms mean Becke's exchange corrections[19] involving the gradient of the density and Vosko, Wilk, and Nusair (VWN) correlation functional,[39] and the last term is the correlation correction of Lee, Yang, and Parr,[20] which includes the gradient of the density. C_i ($i = 1-5$) is the mixing coefficient; for example, (0.5, 0.5, 0.5, 1.0, 1.0) for B2LYP, (0.2, 0.8, 0.72, 1.0, 0.81) for B3LYP,[21] and (0.0, 1.0, 1.0, 1.0, 1.0) for BLYP.

BS calculations for LS states suffer from spin contamination, and spin projection is necessary to eliminate it. We applied our approximate spin projection (AP) scheme.[7,40−42] The total energy is given by the AP scheme as

$$^{LS}E_{AP-X} = {}^{LS}E_X + f_{SC}[{}^{LS}E_X - {}^{HS}E_X] \quad (11a)$$

$$f_{SC} = \frac{[{}^{LS}\langle S^2\rangle_X - S_{min}(S_{min}+1)]}{{}^{HS}\langle S^2\rangle_X - {}^{LS}\langle S^2\rangle_X} \quad (11b)$$

where $^{Y}E_X$ and $^{Y}\langle S^2\rangle_X$ denote the total energy and total angular momentum of the spin state Y by method X (X = UHF and UDFT), respectively. Using the occupation numbers of NOs of UQCISD solutions, we estimated $^{LS}\langle S^2\rangle$ for UQCISD(T) and UCCSD(T) with the following equation[23]

$$^{LS}\langle S^2\rangle = S_{min}(S_{min}+1) + \sum\{1-(T^{\kappa})^2\} \quad (11c)$$

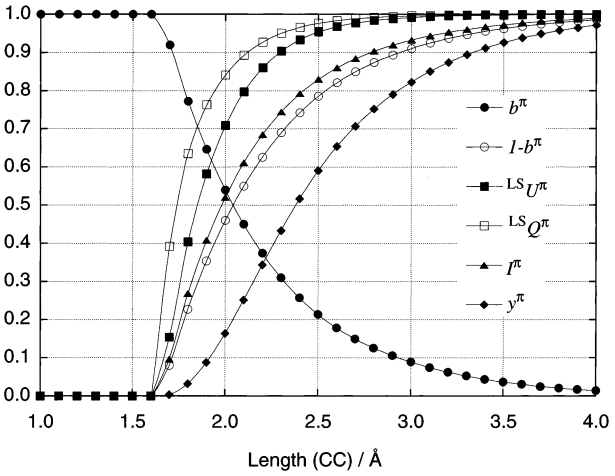

Figure 2. Variations of effective bond order (b^π), the decrease of bond order ($1 - b^\pi$), unpaired electron density ($^{LS}U^\pi$), spin density ($^{LS}Q^\pi$), information entropy (I^π), and diradical character (y^π) for the π bond with the C−C elongation of ethylene.

where S_{min} means the exact quantum number of spin for the LS state. We[3a,7,23] examined the reliability of eq 11 in several reaction systems, showing that it works well for qualitative purposes.

Variations of the Chemical Indices with the C−C Dissociation. To obtain a pictorial understanding of several chemical indices, we have calculated bond orders ($b^\kappa \equiv T^\kappa$), the decrease of bond order ($\Delta b^\kappa = 1 - b^\kappa$), spin density index ($^{LS}Q_a^\kappa$), unpaired electron density ($^{LS}U^\kappa$), information entropy (I_n^κ), and diradical character (y^κ) during the C−C dissociation process of ethylene using the UHF, UB2LYP, UB3LYP, and UBLYP/6-31G* methods. Figure 2 depicts variations of these chemical indices with a change of the π bond length by the R(U)B3LYP/6-31G* method. The functional behaviors of the six indices on R_{C-C} are quite similar among HF, B2LYP, B3LYP, and BLYP (see Supporting Information) except for the instability threshold (R_{IT}^π), when the closed shell pair **1** or **2** splits into the open shell pair **3** or **4**. The critical C−C distances (R_{IT}^π) are 1.3, 1.5, 1.6, and 1.7 Å, respectively. This implies that chemical indices are responsible for several physical contents irrespective of the computational methods, although stable regions of closed shell pairs **1** and **2** are relatively small and large, respectively, for HF and BLYP.

Figure 2 depicts variations of these chemical indices with change of the π bond length by the R(U)B3LYP/6-31G* method. From Figure 2, the $^{LS}Q_a^\kappa$ value sharply increases near the bifurcation point, showing that it is sensitive to the small pair splitting. Its magnitude becomes larger than 0.5 even if the reduction of π orbital overlap via the orbital splitting in **3** is only 0.13, namely, $T^\pi = 0.87$. The similar behavior is also recognized for the $^{LS}U^\pi$ value equivalent to the $\Delta\langle S^2\rangle$ value. It becomes larger than 0.5 if the reduction exceeds the threshold (0.29), namely, $T^\pi \leq 0.71$. As shown in eqs 6 and 7, the $^{LS}Q_a^\kappa$ and $^{LS}U^\pi$ values are closely related to spin correlation. The y^κ value gradually increases with the elongation of the C−C bond and is regarded as a useful index to characterize the strong localization of π electrons. It is only 1% for $T^\pi = 0.87$ and 6% for $T^\pi = 0.71$ and becomes larger than 50% in the weak bond region ($T^\pi \leq 0.27$). It is noteworthy that the oxygenated dipoles such as ozone exhibit 40−50% diradical character under the UHF approximation.[23] The I_n^π and Δb^π values exhibit the intermediate behaviors between the above two extreme indices.

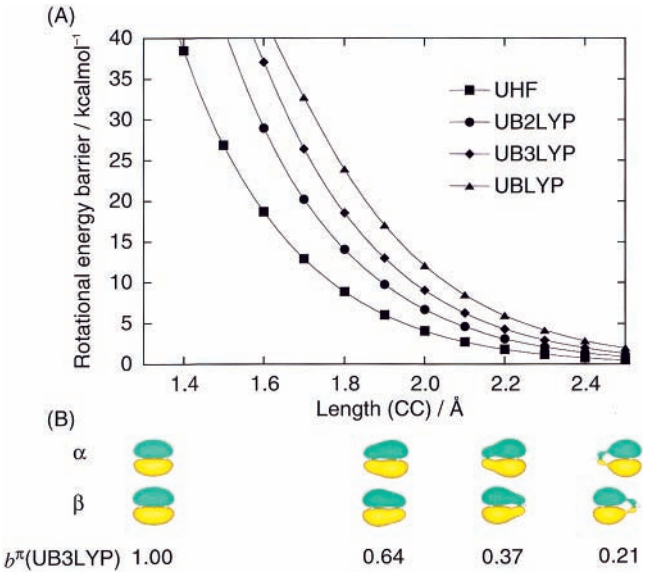

Figure 3. (A) Variations of rotational energy barriers for the π bond with the change of the C−C distance of ethylene. (B) The α and β spin π orbitals and effective bond order (b^π) of ethylene at the equilibrium and C−C elongated ethylene.

The Δb^π value linearly increases with the decrease of the overlap. The I_n^π value exhibits a similar functional behavior. It could be regarded as a useful index to diagnose the bond nature. The bond order and information entropy are the measures of electron delocalization, namely, the strength of covalent bonds.

To elucidate the interrelationship between chemical index and nonstereospecificity, we have calculated the rotational energy barriers (ΔE_{rot}) for the internal rotation around the C−C bond, namely, from planar ethylene to perpendicular ethylene.

$$\Delta E_{rot} = E(\text{perpendicular}) - E(\text{planar}) \qquad (12)$$

Figure 3A illustrates variations of the barriers with the change of the C−C distance. The rotational barriers decrease with the increase of the C−C distance (R). They also increase depending on the computational methods in the following order: ΔE_{rot}(BLYP) > ΔE_{rot}(B3LYP) > ΔE_{rot}(B2LYP) > ΔE_{rot}(HF). It becomes smaller than 10 kcal mol^{-1} if R exceeds the threshold value (2.0 Å) even at the UB3LYP level or if b^π becomes smaller than 0.5. Figure 3B illustrates variations of shapes of π orbital during the C−C dissociation by UB3LYP. The α and β spin MOs are equivalent at $R = 1.3$ Å, showing the closed shell orbital configuration **1** or **2**, respectively. The decrease of the rotational energy barriers is parallel to the localization of π electrons at the left and right carbon atoms in Figure 3B. Conversely, Figure 3B clearly shows the bond formation in the thermally allowed association process of triplet methylenes as illustrated in Scheme 1, where $\delta\cdot$ means the partial localization of electron and R = H. On the other hand, such a stable C−C double bond is hardly formed if R = *tert*-butyl because of steric repulsion. Very recently, it was indeed found that phenalenyl radical (**6**) with three *tert*-butyl groups forms the antiferromagnetic dimer (**7**) in the crystalline state (Scheme 1).[43,44]

As displayed in Figure 4, general trends of variations of the chemical indices for the C−C σ bond[44] in the course of the C−C dissociation or association are quite similar to those of the π bond. However, their variations are not so sharp as compared with these of the π bond. This is attributable to the

SCHEME 1

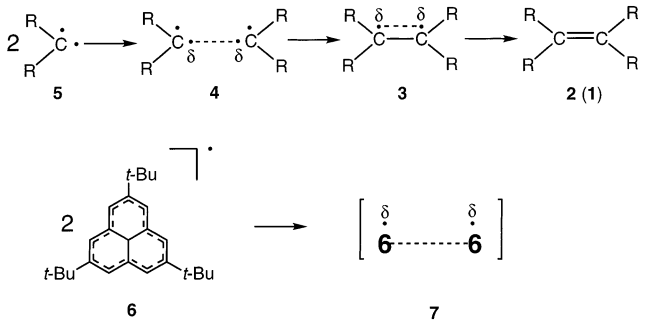

fact that the pσ−pσ orbital overlap is larger than the pπ−pπ one, and pσ bond is stronger than the pπ bond in the long C−C bond region (R > 1.5 Å). The bond natures revealed by the chemical indices are largely dependent on the computational methods. Chemical pictures of the σ bond at R = 2.5 Å are quite different between UHF and UBLYP. Moreover, significant differences between UB3LYP and UBLYP are also recognized, for example, no diradical character by UBLYP. Because the $\pi\sigma-\pi\sigma$ bond is formed between 4π and 2π bonds in the Diels−Alder reactions, chemical indices behave differently by different computational methods in the transition region; 1.8 ≤ R ≤ 2.8 Å should be very important for qualitative understanding of the nature of σ bonds at the TS of the reactions. The singlet diradical dimer (**7**) of **6** is an interesting target to examine different behaviors of the $\pi\sigma-\pi\sigma$ bond by the BS solutions.[43]

Theoretical Calculations of the Diels−Alder Reactions

BS Calculations. Figure 5 illustrates the concerted and diradical stepwise pathways for the Diels−Alder reaction of butadiene and ethylene. The geometries of the CTSs and NTSs for the parent system (**I**)[45−48] have been reported by many groups.[3−7] Here, the R(U)B3LYP/6-31G* geometry parameters optimized by Houk and his collaborators[3a] were employed. Calculations on TSs were limited to CTS, anti NTS, and gauche-out NTS because of the difficulty in location of the gauche-in diradical TS.[3a] The diradical intermediate (DI) was also limited to the anti conformation here for the same reason. For all structures, zero-point vibrational energy corrections were performed.

We first performed the RHF and UHF calculations using 6-31G* for the CTS, anti NTS, and gauche-out NTS, respectively. The calculated results are shown in Table 1. The activation barriers for the anti and gauche-out NTSs are lower by about 25 kcal mol^{-1} than that of the CTS at the UHF/6-31G* level. This trend is the same in the case of the UMINDO/3 calculations by Dewar et al.[3] The UHF solutions for the NTSs exhibit strong diradical characters arising from BS. APUHF provided 8.8 and 9.1 kcal mol^{-1} activation barrier for the anti and gauche-out NTSs, respectively. The greater stability of the NTSs with nonnegligible diradical character than the CTS is a characteristic of HF approximations, because both UHF and APUHF solutions partially include the nondynamical correlation corrections for the NTSs with radical character via the symmetry breaking of frontier orbitals.

Next, we performed the QCISD(T)[11] and CCSD(T)/6-31G*[10] calculations of the CTS and NTSs. In Table 1, the trend at the HF level is reversed after the dynamical correlation correction by QCISD(T) and CCSD(T). This implies that the dynamical correlation correction is crucial for the well-balanced estimation of the relative energy between the CTS and the NTSs. This is the reason that the BS hybrid DFT including correlation functionals works well for locations of them.

The activation barrier for the CTS by the CCSD(T)/6-31G* is close to the experimental value (27.5 ± 2 kcal mol^{-1}).[48] The AP procedure reduces the activation barrier for the anti and gauche-out NTSs by about 8 kcal mol^{-1}. After AP, the energy difference (4.4 kcal mol^{-1}) between the CTS and the NTSs is also in the range of the experimental estimation, 2−7 kcal mol^{-1},[46] and the DI is more stable than the NTSs by 1−2 kcal mol^{-1}. The BS approach followed by the correlation correction at the CCSD(T) level and spin projection has provided a reasonable description of both CTS and NTS.

SA Calculations. The SA multiconfiguration (MC) approach is feasible for relatively small systems to examine the above question. The RHF solution for the CTS involves the triplet instability, and the UHF solution is more stable. The NO analysis of the UHF solution has provided the UHF NO (UNO) for the CTS as shown in Table 2.[23] The occupation numbers of other NOs are almost 2.0 (closed shell) or 0.0 (vacant) for both CTS and NTSs. We performed the CASCI by using the six UNO six electron {6, 6} for both TSs. In Table 2, the occupation numbers of highest occupied molecular orbital (HOMO) and lowest unoccupied molecular orbital (LUMO) are largely improved after UNO CASCI. UNO CASCI results are not so different after the refinement by CASSCF.

The activation barriers for the CTS, anti, and gauche-out NTSs by UNO CASCI {6, 6} and CASSCF {6, 6} are shown in Table 1. The CTS is more stable than the NTSs by 1.5−2.5 kcal mol^{-1}. The DI is more stable than the NTSs by 0.5−6.4 kcal mol^{-1}. This is reasonable as compared with the CCSD(T) result. However, the heat of formation is much smaller than the experimental value, 38.4 kcal mol^{-1}. The results by UNO CASCI {6, 6} and CASSCF {6, 6} suggest that the UNOs are not so different from NOs of CASSCF. The UNO analyses can be used for large systems, for which the CASSCF calculations are impossible as shown below.

The activation barrier for the CTS at the CASSCF {6, 6} level is too large, as compared with the experiment,[48] while the heat of formation is too small. This clearly indicates the necessity of dynamical correlation correction. MRMP2 calculations[49] based on CASSCF {6, 6} solution were performed to estimate such correction. Because UNO CASCI {6, 6} was a good approximation to CASSCF {6, 6}, the MP2 calculations starting from the UNO CASCI {6, 6} (CASMP2(CI) {6, 6})[23] were also performed. The activation barrier heights by CASMP2-(CI) and MRMP2 are close to that by BLYP. The heats of formation at the MP2 level are in accord with the experiments. The MP2 calculations clearly demonstrated the necessity of dynamical correlation corrections even for the CTS and reactants. The computational results are not so different between MRMP2 and CASMP2(CI). This means that CASMP2(CI) is applicable to relatively large systems for qualitative purpose, leaving out the time-consuming CASSCF process for such systems.

The activation barriers for the CTS by MRMP2 and CASMP2-(CI)/6-31G* are lower than the experiment.[45] The barrier for the CTS by present RMP2/6-31G* calculation is similar to the CASMP2(CI) value. However, the RMP2 energy seems too deep because of triplet instability of the RHF solution.[7] Because the UHF solutions are available for the NTSs, the UMP2 and APUMP2 calculations are also feasible. The APUMP2 values are larger than the APUCCSD(T) values. The present results may indicate that both single and MR MP2 are still insufficient for dynamical correlation correction as compared with QCISD(T) and CCSD(T). This implies that the MR CC approach is desirable for a quantitative purpose.[8]

TABLE 1: Relative Energies[a] for the Diels−Alder Reaction of Butadiene and Ethylene (System I) by the Post Hartree−Fock and MR Methods

	HF	MP2	QCISD(T)	CCSD(T)	UNO CASCI (CASSCF)	CASMP2(CI) (MRMP2)	exp
butadiene + ethylene	0.0	0.0	0.0	0.0	0.0	0.0	
CTS	46.6	20.4	27.6	27.6	40.5(45.1)	19.8(22.4)	27.5 ± 2
anti NTS	21.3(8.8)[b]	49.9(42.0)[b]	40.7(32.1)[b]	40.7(32.0)[b]	42.0(46.6)	26.0(28.6)	
gauche-out NTS	21.8(9.1)[b]	51.2(44.1)[b]	42.0(33.8)[b]	42.0(33.7)[b]	43.0(47.7)	27.5(30.1)	
DI	5.7(4.9)[b]	36.3(35.4)[b]	31.9(30.8)[b]	32.0(31.0)[b]	40.5(41.3)	27.1(27.0)	
cyclohexene	−36.5	−46.3	−40.6	−40.6	−5.6(−0.9)	−41.1(−38.7)	−38.4

[a] Relative energies are in kcal mol^{-1} and include zero-point corrections. [b] Values in parentheses are after spin correction.

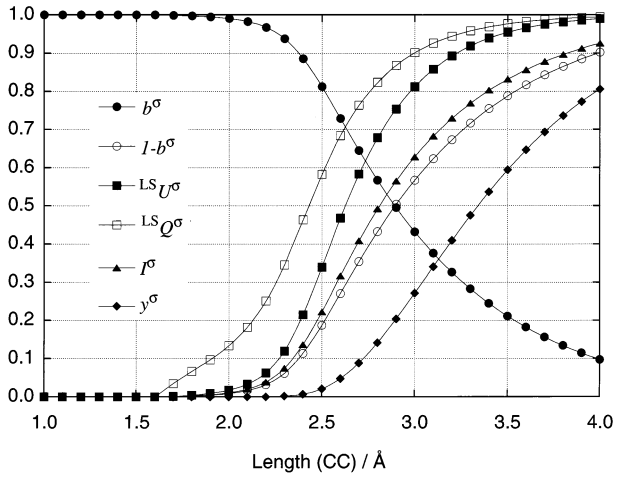

Figure 4. Variations of effective bond order (b^σ), the decrease of bond order ($1 - b^\sigma$), unpaired electron density ($^{LS}U^\sigma$), spin density ($^{LS}Q^\sigma$), information entropy (I^σ), and diradical character (y^σ) for the σ bond with the C−C elongation of ethylene.

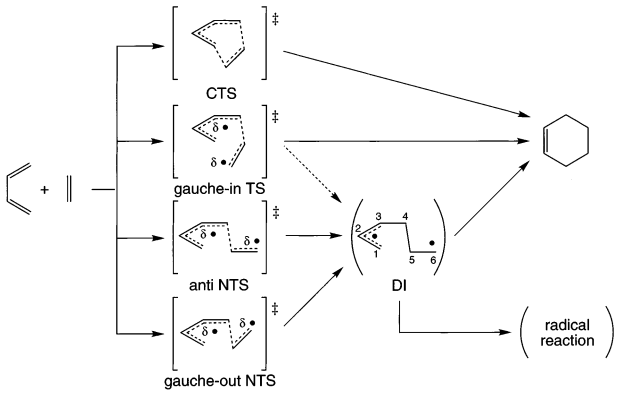

Figure 5. Schematic illustration of the concerted and stepwise pathways for the Diels−Alder reaction of butadiene and ethylene.

Hybrid Density Functional Calculations. Pure and hybrid DFT are often utilized for locations of the TSs of large systems.[3,14−18] It is very interesting to elucidate its reliability and applicability as compared to the preceding post HF calculations.

Table 3 summarizes the calculated results. BLYP gives an activation energy for the CTS that is lower than the experiment (27.5 kcal mol^{-1}), like the LDF/DZVP calculations.[50] The energy gap between the CTS and the NTSs is 9−11 kcal mol^{-1}, which is larger than the experimental estimation (2−7 kcal mol^{-1}).[46] This may be attributable to overstabilization of the CTS at the BLYP/6-31G* level. The UBLYP solution for the anti NTS reduces to the RBLYP, so that the diradical character of the anti NTS of the Diels−Alder reaction is quenched with BLYP. The same conclusion was presented for the Cope rearrangement reaction by Steroverov and Davidson.[22] However, the UBLYP solutions are more stable for the gauche-out NTS and DI than the RBLYP solutions. The diradical character is significant for the species.

The B3LYP/6-31G* calculations predicted that the activation barrier for the CTS is 24.8 kcal mol^{-1}. The RB3LYP solution is stable for the CTS geometry but unstable at both anti and gauche-out NTS geometries. The energy gap between the CTS and the NTSs is 5−6 kcal mol^{-1}, in good agreement with the experimental value.[46] The inclusion of the 20% HF exchange at the UB3LYP level changes the nature of the chemical bonds at the anti NTS, and the diradical character becomes non-negligible as discussed below. The heat of formation is also consistent with the experiment.

The B2LYP calculations involving the 50% HF exchange were also performed. The activation barriers show that the B2LYP method overestimates the diradical character of the NTSs, because of the inclusion of too much HF exchange functional. The heat of formation by B2LYP becomes larger than the experimental value.

The results are highly dependent on the weight (w_{HF}) of the HF exchange. The B2′LYP calculations with $w_{HF} = 40$ and 30% were performed for comparison. In Table 3, the energy difference between the CTS and the anti NTS by UB2′LYP ($w_{HF} = 30\%$) is 1.3 kcal mol^{-1}. Both the activation barrier and the energy difference are consistent with the CCSD(T) results. Table 2 summarizes the occupation numbers of six active orbitals for both anti and gauche-out NTSs by hybrid DFT methods, together with the QCISD method. The occupation numbers by B2′LYP are close to those of CASSCF. Therefore, B2′LYP would be a good approximation to MR CC.

Hybrid DFT methods, particularly UB3LYP and UB2′LYP ($w_{HF} = 30\%$), reproduce the activation barrier heights and energy differences between the CTS and the NTSs for the Diels−Alder reaction, obtained from UCCSD(T) and UQCISD-(T) methods. Hybrid DFT procedure can be used as a practical alternative to the latter approaches. Later in this paper, we will clarify why hybrid DFT works well on the basis of chemical indices. Hybrid DFT is applicable to larger systems for which CASPT2 or MRMP2 and MR CC are not feasible. The Diels−Alder and the Cope rearrangement reactions involving phenyl substituents are such examples.

Stabilization of NTS by Phenyl Groups. The energy differences between CTS and NTSs are sensitive to substituents introduced at reaction sites. We have examined the Diels−Alder reactions between phenyl-substituted dienes and olefins. The reactions examined here are (**II**) 1-phenylbutadiene and ethylene, (**III**) butadiene and styrene, and (**IV**) 1-phenylbutadiene and styrene. We have taken up exo TSs in all systems, where the phenyl group of styrene sits away from the conjugated system of diene. In addition to the exo and endo stereochemistry, there are two possible regiospecific approaches for the system **IV**, depending on the orientation of the two phenyl groups. Because the cycloaddition of 1-substituted diene and monosubstituted

TABLE 2: Occupation Numbers of NOs, Information Entropy, and Polyradical Characters for the CTS, NTS, and DI of the Diels−Alder Reaction of Butadiene and Ethylene (System I) by the Post Hartree−Fock and Hybrid UDFT Methods

	method	HOMO − 2	HOMO − 1	HOMO	LUMO	LUMO + 1	LUMO + 2	I_n (I_{HOMO})	U_n ($^{LS}U_{HOMO}$)	Y_n (y_{HOMO})
CTS	UHF	1.942	1.804	1.741	0.259	0.196	0.058	0.20(0.30)	0.31(0.45)	0.02(0.04)
	UNO CASCI	1.946	1.878	1.856	0.145	0.123	0.054	0.13(0.17)	0.20(0.27)	0.01(0.01)
	CASSCF	1.946	1.880	1.862	0.139	0.120	0.053	0.12(0.16)	0.20(0.26)	0.01(0.01)
	QCISD	1.941	1.907	1.900	0.086	0.077	0.047	0.10(0.12)	0.15(0.18)	0.00(0.01)
	UDFT[a]	2.000	2.000	2.000	0.000	0.000	0.000	0.00(0.00)	0.00(0.00)	0.00(0.00)
anti NTS	UHF	1.964	1.893	1.271	0.729	0.107	0.036	0.32(0.78)	0.40(0.93)	0.17(0.50)
	UNO CASCI	1.949	1.906	1.525	0.477	0.093	0.050	0.24(0.54)	0.33(0.73)	0.06(0.18)
	CASSCF	1.949	1.907	1.547	0.456	0.092	0.050	0.23(0.51)	0.33(0.70)	0.05(0.16)
	QCISD	1.934	1.911	1.442	0.544	0.074	0.049	0.27(0.62)	0.36(0.80)	0.09(0.26)
	UB2LYP	1.990	1.972	1.455	0.545	0.028	0.010	0.22(0.61)	0.29(0.79)	0.08(0.25)
	UB2′LYP ($C_1 = 0.4$)	1.993	1.979	1.507	0.493	0.021	0.007	0.20(0.55)	0.27(0.74)	0.06(0.19)
	UB2′LYP ($C_1 = 0.3$)	1.995	1.986	1.574	0.426	0.014	0.005	0.17(0.49)	0.24(0.67)	0.05(0.14)
	UB3LYP	1.997	1.992	1.676	0.324	0.008	0.003	0.13(0.38)	0.19(0.54)	0.02(0.07)
	UBLYP	2.000	2.000	2.000	0.000	0.000	0.000	0.00(0.00)	0.00(0.00)	0.00(0.00)
gauche-out NTS	UHF	1.960	1.891	1.257	0.743	0.109	0.040	0.32(0.79)	0.41(0.93)	0.18(0.52)
	UNO CASCI	1.947	1.905	1.508	0.494	0.095	0.052	0.24(0.55)	0.34(0.74)	0.07(0.19)
	CASSCF	1.946	1.906	1.530	0.473	0.093	0.052	0.24(0.53)	0.33(0.72)	0.06(0.17)
	QCISD	1.933	1.910	1.422	0.563	0.075	0.051	0.28(0.64)	0.36(0.82)	0.10(0.28)
	UB2LYP	1.989	1.971	1.434	0.566	0.029	0.011	0.23(0.63)	0.30(0.81)	0.09(0.27)
	UB2′LYP ($C_1 = 0.4$)	1.992	1.979	1.483	0.517	0.021	0.008	0.20(0.58)	0.28(0.77)	0.07(0.22)
	UB2′LYP ($C_1 = 0.3$)	1.994	1.985	1.547	0.453	0.015	0.006	0.18(0.51)	0.25(0.70)	0.05(0.16)
	UB3LYP	1.996	1.992	1.644	0.356	0.008	0.004	0.14(0.41)	0.20(0.59)	0.03(0.09)
	UBLYP	2.000	1.999	1.948	0.052	0.001	0.000	0.02(0.06)	0.03(0.10)	0.00(0.00)
DI	UHF	1.996	1.895	1.079	0.921	0.105	0.004	0.36(0.94)	0.40(0.99)	0.28(0.84)
	UNO CASCI	1.992	1.903	1.164	0.837	0.097	0.008	0.33(0.87)	0.39(0.97)	0.23(0.68)
	CASSCF	1.981	1.904	1.175	0.825	0.096	0.019	0.33(0.86)	0.40(0.97)	0.22(0.66)
	QCISD	1.951	1.907	1.113	0.872	0.079	0.029	0.36(0.91)	0.41(0.99)	0.26(0.78)
	UB2LYP	1.998	1.967	1.139	0.861	0.033	0.002	0.31(0.89)	0.35(0.98)	0.24(0.73)
	UB2′LYP ($C_1 = 0.4$)	1.999	1.974	1.157	0.843	0.026	0.001	0.30(0.88)	0.34(0.98)	0.23(0.69)
	UB2′LYP ($C_1 = 0.3$)	1.999	1.981	1.181	0.819	0.019	0.001	0.29(0.86)	0.34(0.97)	0.22(0.65)
	UB3LYP	1.999	1.987	1.218	0.782	0.013	0.001	0.28(0.83)	0.33(0.95)	0.20(0.58)
	UBLYP	1.999	1.995	1.348	0.652	0.005	0.001	0.24(0.71)	0.30(0.88)	0.13(0.38)

[a] DFT = B2LYP, B2′LYP, B3LYP, and BLYP.

TABLE 3: Relative Energies[a] for the Diels−Alder Reaction of Butadiene and Ethylene (System I) by the Hybrid DFT Methods

	B2LYP	B2′LYP ($C_1 = 0.4$)	B2′LYP ($C_1 = 0.3$)	B3LYP	BLYP	exp
butadiene + ethylene	0.0	0.0	0.0	0.0	0.0	
CTS	29.4	28.2	26.9	24.8	23.0	27.5 ± 2
anti NTS	32.5(24.7)[b]	33.6(26.5)[b]	34.4(28.2)[b]	34.3(29.4)[b]	32.5	
gauche-out NTS	33.4(25.8)[b]	34.5(27.6)[b]	35.3(29.1)[b]	35.3(30.2)[b]	33.6(32.7)[b]	
DI	21.9(20.8)[b]	24.5(23.3)[b]	26.9(25.7)[b]	28.9(27.6)[b]	33.0(31.2)[b]	
cyclohexene	−43.3	−40.5	−37.7	−36.6	−29.3	−38.4

[a] Relative energies are in kcal mol^{-1} and include zero-point corrections. [b] Values in parentheses are after spin correction.

olefin generally gives more of the ortho adduct,[51] we have investigated the ortho reaction mode only. The RB3LYP energy gradient technique was utilized for determination of the reactants and CTS, while the full geometry optimizations of the anti NTS and anti DI were carried out by the UB3LYP method. The relative energies for them were also calculated by HF, B2LYP, and BLYP, assuming the B3LYP optimized geometries. Table 4 summarizes the calculated results for the systems **II**−**IV**. Figure 6 shows the variations of activation barriers with the introduction of phenyl group(s).

The activation barriers for the anti NTS by B3LYP/6-31G* decrease with the introduction of phenyl group(s), while those of the CTS exhibit relatively small variation in energy with it, as shown in Figure 6. The stabilization for the DI by phenyl groups is also significant as shown in Table 4. The differences of the barriers between the CTS and the NTS by B3LYP are 9.5, 6.0, 2.3, and 2.5 kcal mol^{-1} for **I**−**IV**, respectively. After the AP procedure for the UB3LYP/6-31G* solutions of the NTSs, they become 4.6, 1.2, −1.6, and −0.7 kcal mol^{-1}, respectively. Because of the nonnegligible diradical character for the NTSs of **III** and **IV**, they become more stable than nonradical CTSs. For lucid understanding of this reversion, Figure 7 illustrates the optimized geometries of the CTS and anti NTS of **IV**.[52] The π HOMO of the NTS is stabilized by the delocalization over the phenyl group because of the almost planar conformation (twisted angles (a) of phenyl groups are small), while such efficient conjugation by phenyl groups for the CTS conflicts with the formation of the new σ bond due to the rehybridization of the terminal carbon atoms from sp^2 to sp^3 (large twisted angles). A highly asymmetric structure is, therefore, given to the ortho CTS by the introduction of two phenyl groups as illustrated in Figure 7.

Information Entropy, Unpaired Electron Density, and Polyradical Characters

Parent System. Unpaired electron density (U), information entropy (I), and polyradical character (y) are useful indices for the investigation of bonding characteristics as shown in Figures 2 and 3. Using the occupation numbers, these values for the Diels−Alder reaction of the parent system (**I**) can be estimated with eqs 3−9. The occupation numbers and these indices are summarized in Table 2.

TABLE 4: Relative Energies[a] for the Diels−Alder Reactions of Phenyl Derivatives (Systems II−IV) by the Hybrid DFT Methods

system		HF	B2LYP	B3LYP	BLYP
II	1-phenylbutadiene + ethylene	0.0	0.0	0.0	0.0
	CTS	47.2	29.9	25.7	24.3
	anti NTS	9.7(−13.0)[b]	29.9(21.1)[b]	31.7(26.9)[b]	29.5
	DI	−6.5(−7.5)[b]	18.4(17.6)[b]	25.9(24.8)[b]	29.9(28.5)[b]
III	butadiene + styrene	0.0	0.0	0.0	0.0
	CTS	48.7	29.9	25.0	23.1
	anti NTS	6.7(−16.5)[b]	26.0(17.4)[b]	27.3(23.4)[b]	24.3
	DI	−11.9(−12.7)[b]	12.7(11.9)[b]	20.4(19.4)[b]	24.3(22.9)[b]
IV	1-phenylbutadiene + styrene	0.0	0.0	0.0	0.0
	CTS	47.7	28.0	23.0	21.0
	anti NTS	−3.9(−39.3)[b]	24.2(15.3)[b]	25.5(22.3)[b]	22.2
	DI	−24.1(−25.0)[b]	9.2(8.6)[b]	17.3(16.5)[b]	21.1(20.0)[b]

[a] Relative energies are in kcal mol^{-1} and include zero-point corrections. [b] Values in parentheses are after spin correction.

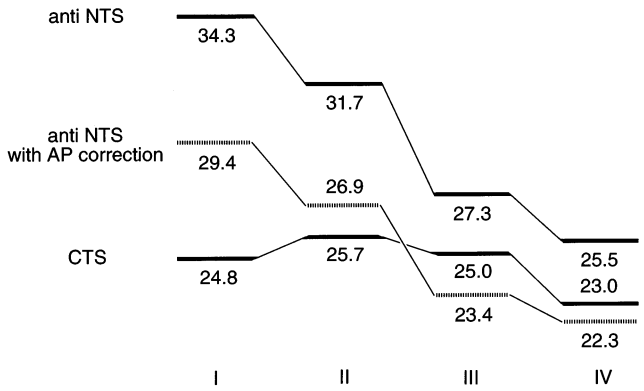

Figure 6. Variations of activation energy barriers for the CTS and anti NTS of the Diels−Alder reactions of phenyl derivatives (systems **I**−**IV**) by B3LYP.

The diradical characters (y_{HOMO}) for the anti and gauche-out NTSs by HF approximation are close to those (50%) of oxygenated dipoles such as ozone.[23] The y_{HOMO} values by B2LYP become one-half as compared with the HF value. This is a general trend under DFT approximation, namely, the instability in chemical bonds is relaxed with the change from UHF to UDFT. The diradical character by UBLYP is very small.

To clarify possible reasons of the above drastic change, we have performed the NO analyses of the QCISD, UNO CASCI, and CASSCF solutions for both CTS and NTSs. The occupation numbers are shown in Table 2. The *n* values of LUMO by UHF become smaller after correlation correction by QCISD, showing that the overestimation of the diradical character y_{HOMO} is improved. On the other hand, the nonzero *n* values of LUMO by QCISD and CASSCF in turn indicate the importance of dynamical correlation correction for the closed shell RHF solution. If such contributions are included in DFT orbitals, the *n* value for LUMO should be reduced or become zero, and the occupation numbers of bonding DFT NO (DNO) are larger than those of UNO. Because n_{LUMO} for the CTS by QCISD (0.09) is reduced to zero by DFT, n_{LUMO} for the NTSs for the best UDFT would reproduce the QCISD, UNO CASCI, and CASSCF values. UB2′LYP or UB3LYP is the best alternative to QCISD-(T) or CCSD(T), in accord with the energetics.

The above successful modification of B2LYP suggests a possibility of searching the best hybrid DFT for a system under investigation. Very recently,[53] we have shown that UNO analysis[23] can be used to estimate the mixing coefficient (C_1) of the HF exchange potential for hybrid DFT. For example, the UNO CAS is taken to be six π orbital and six electron for the CTS and NTSs of the Diels−Alder reaction. The average normalized indices are defined to investigate the degree of the nondynamical correlation correction for DFT by

$$I_n = \frac{1}{N}\sum_{i=1}^{N} I_n^i \tag{13a}$$

$$U_n = \frac{1}{2N}\sum_{i=1}^{2N} U^i \tag{13b}$$

$$Y_n = \frac{1}{N}\sum_{i=1}^{N} y^i \tag{13c}$$

where $N = 3$. The chemical indices are used to judge the mixing coefficients of the HF exchange potential.[53] For the purpose, the normalized I_n, U_n, and Y_n values are calculated using the occupation numbers of NOs. The results are summarized in Table 2. All of the normalized indices for the CTS are zero for the UDFT solutions, but those for UHF are not zero due to the triplet instability of RHF solution. Nonzero values are also given for UNO CASCI and CASSCF because of dynamical correlation corrections. For the NTSs and DI, the interrelationship, $Y_n < I_n < U_n$, is recognized for each computational method. This is consistent with the general trend in Figure 2. Judging from the I_n values, the chemical bonds at the CTS and NTSs for the Diels−Alder reaction between butadiene and ethylene are regarded as in the strong and moderate bonding regions, respectively.[7] Moreover, all chemical indices indicate that the anti NTS has smaller diradical character than the gauche-out NTS. The UNO analysis shows that B2′LYP ($C_1 = 30\%$) or B3LYP ($C_1 = 20\%$) is utilized as an alternative to QCISD.

The I_n value for the DI by UHF suggests that B2′LYP ($C_1 = 30\%$) is a better hybrid DFT for the DI,[53] although variational determination of C_1 would be the best procedure for quantitative purpose. The diradical character (y_{HOMO}) of the DI exceeds 80% at the HF level, like in the case of trimethylene diradical.[23] The effective bond orders for the DI become in the range $0.08 \le b^{\pi}_{HOMO} \le 0.35$, by the quantum chemical methods employed here as shown in Table 2, while those for the NTSs are $0.26 \le b^{\pi}_{HOMO} \le 1.00$. We can understand the flexibility of the system under investigation using these values. For example, judging from the b^{π}_{HOMO} (UB3LYP) values, the C−C bond rotation will not occur until the NTSs ($b^{\pi}_{HOMO} = 0.64-0.68$) collapse into the DI ($b^{\pi}_{HOMO} = 0.22$)[54] as shown in Figure 3, while extremely rigid structure ($b^{\pi}_{HOMO} = 1.00$) for the concerted pathway will ensure the retention of the stereochemistry of the system.

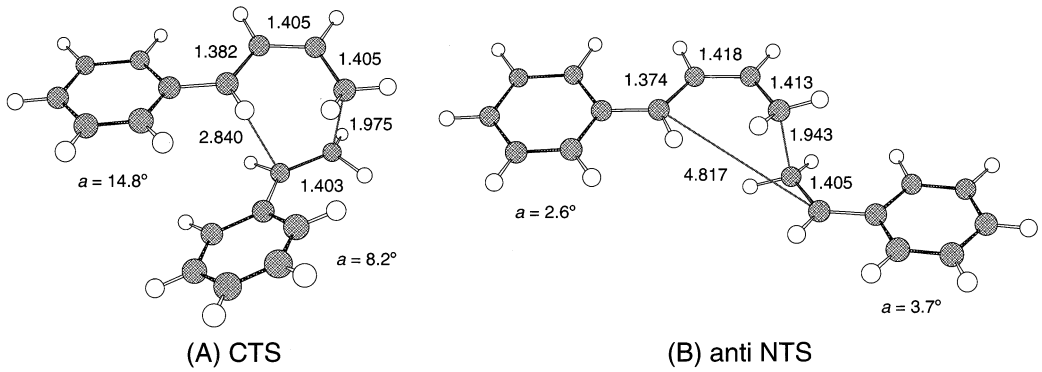

Figure 7. Schematic illustration of the optimized geometries of the CTS and anti NTS for the Diels−Alder reaction between 1-phenylbutadiene and styrene (**IV**) by the B3LYP method.

Substituted Systems. The NO analyses of the BS solutions for the phenyl-substituted systems **II**−**IV** were performed to elucidate their NOs and the occupation numbers. From the UNO results, the CAS spaces are {12, 12} for **II** and **III**, while they are {18, 18} for **IV**.[55] However, the CAS is reduced to {4, 4} even for the anti NTS by selecting LUMOs with $n_{\mathrm{LUMO}+i} \geq 0.005$ under the UB3LYP approximation.[55] The UBLYP solution for the anti NTS reduces to the RBLYP one. The quenching of the diradical character by BLYP is a characteristic difference from B3LYP, although both methods indicate the diradical character for the DI.

The n_{LUMO} values for the anti NTS and DI of **II**−**IV** are not so different from those of the parent system (**I**) at each computational level.[56] However, the shapes of NOs should be different because of the introduction of phenyl groups. Fortunately, UNO CASCI {6, 6} and CASSCF {6, 6} calculations for **I** have revealed that UNOs are good approximations to CASSCF NOs (CNO). If we can expect the same situation even for large systems, UNOs for **II** (**III**) and **IV** are similar to CNOs of CASSCF {12, 12} and {18, 18}, respectively. We here depict HOMO (HONO) and LUMO (LUNO) for **II**−**IV** by UHF for pictorial understanding of diradical stabilization as shown in Figure 8. The HONO and LUNO for **II** are delocalized over the phenyl ring of 1-phenylbutadiene, showing the stabilization of π LUMO. Similarly, HONO and LUNO for **III** are delocalized over the phenyl ring of styrene, leading to the same diradical stabilization. The HONO and LUNO for **IV** are delocalized over both phenyl groups, showing the synergic stabilization. This is the reason that the anti NTS becomes favorable for **III** and **IV**.

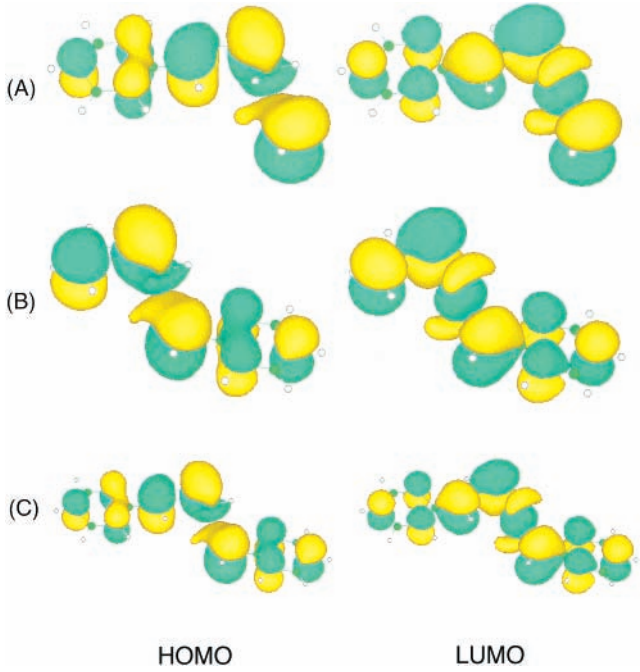

Figure 8. HOMO and LUMO of the anti NTS for the Diels−Alder reactions between phenyl-substituted diene and olefin; (A) 1-phenylbutadiene plus ethylene (**II**), (B) butadiene plus styrene (**III**), and (C) 1-phenylbutadiene plus styrene (**IV**).

Discussions and Concluding Remarks

NO Analysis and Chemical Indices. Systematic comparisons between the BS and the SA approaches to transition states were conducted using the chemical indices spin density (Q), unpaired electron density (U),[22,24,25] effective bond order (b), information entropy (I),[26−29] and diradical character (y).[23] They are defined by the occupation numbers of NOs by both BS and SA methods. The functional behaviors of these indices during the C−C dissociation process of ethylene or the least motion association reaction of triplet methylenes were examined in order to elucidate different characteristics among the BS methods, namely, UHF, UB2LYP, UB3LYP, and UBLYP. UHF and UBLYP overestimate and underestimate the diradical character of π and σ bonds of dissociated ethylene, while UB3LYP provides the reasonable results.

The RB3LYP method is useful for the location of CTSs, while the UB3LYP method is reliable for search of NTSs with diradical character. The relative stability between the CTS and the NTSs for the Diels−Alder reaction of butadiene and ethylene by B3LYP/6-31G* exhibits the same trend concluded by the post Hartree−Fock methods such as QCISD(T), CCSD(T), and the MR perturbation methods. This may indicate that the hybrid DFT (B3LYP) can be used for relatively large systems as a practical alternative to the CC method.

NO analyses of UHF and UDFT solutions were performed to elucidate the nature of the chemical bonds at TSs. The information entropy and other related indices were calculated using the occupation numbers of NOs. These values are useful to analyze the instability of MOs at TSs, giving a useful criterion for selection of hybrid DFT methods such as B2LYP, B2′LYP, and B3LYP to obtain well-balanced descriptions of nonradical and radical states. The AP procedure for UB2LYP, UB2′LYP, and UB3LYP for NTSs is crucial for improvement of the activation barrier. UB2′LYP (C_1 = 30%) followed by AP reproduces the computational results from UCCSD(T) for the Diels−Alder reaction between butadiene and ethylene.

The MR treatments[32] are desirable for refinements of BS hybrid DFT and/or density matrix functional theory (DMFT).[57−59] UNO and DNO CASCI are utilized as an alternative to CASSCF

TABLE 5: Activation Enthalpies[a] for the Cope Rearrangements of Phenyl-Substituted 1,5-Hexadienes by the Hybrid DFT Methods

substituents		HF	B2LYP	B2′LYP ($C_1 = 0.4$)	B2′LYP ($C_1 = 0.3$)	B3LYP	BLYP	exp
none	CTS	55.6	40.2	38.0	35.8	33.2	30.9	33.5 ± 0.5
2-phenyl	CTS	55.9	37.8	35.5	33.3	30.4	27.6	
	NTS	19.1(3.5)[b]	31.8(23.8)[b]	32.1(25.3)[b]	31.9(26.7)[b]	30.3(28.0)[b]	28.5	29.3 ± 1.6
	DI	4.9(1.0)[b]	24.6(21.3)[b]	26.7(23.2)[b]	28.4(24.9)[b]	29.4(25.8)[b]	31.9(29.0)[b]	
2,5-diphenyl	CTS	53.9	33.3	30.8	28.3	25.1	22.1	
	NTS	7.8(−14.4)[b]	27.2(19.7)[b]	27.5(21.6)[b]	26.9(23.2)[b]	24.8(24.4)[b]	21.5	21.3 ± 0.3
	DI	−12.0(−14.6)[b]	16.1(14.4)[b]	18.5(16.7)[b]	20.3(18.5)[b]	21.3(19.4)[b]	22.8(20.9)[b]	

[a] Activation enthalpies are in kcal mol^{-1} and include thermal correction. [b] Spin-corrected values are in parentheses.

for MR(CAS) DFT. The merit of hybrid DFT methods followed by AP is their applicability to large systems, for which CASSCF-based calculations are difficult. The chemical indices expressed by the occupation numbers of NOs by resulting BS hybrid DFT are useful for understanding of the nature of the chemical bonds from the same theoretical viewpoint as that of SA CASCI(SCF).

Diradical Stabilization and Comparison with the Cope Rearrangement. The present B3LYP calculations show that two phenyl groups reduce the activation barrier for the anti NTS of the Diels−Alder reaction by 7.1 kcal mol^{-1} because of radical stabilization. Doering et al.[60] have pointed out that two phenyl groups in active positions of hexa-1,5-diene appear to lower the energy of the transition region by 8.8 kcal mol^{-1} (4.4 kcal mol^{-1} per phenyl group). Recent B3LYP/6-31G* calculations[61] for the Cope rearrangement of phenyl-substituted 1,5-hexadiene have indeed demonstrated the stabilization. Previous CASSCF/3-21G calculations by Li and Houk[3f] indicated that cyclic and linear NTSs for butadiene dimerization are lower by 1.3 and 2.6 kcal mol^{-1}, respectively, than CTS; note that the same calculation predicts the greater stability of the CTS than the anti NTS by 2−3 kcal mol^{-1} for the Diels−Alder reaction between butadiene and ethylene. The energy gap between the CTS and the NTS for the parent reaction is 1.5 kcal mol^{-1} by the present UNO CASCI and CASSCF, while it becomes 6.2 kcal mol^{-1} by CASMP2(CI) and MRMP2. The dynamical correlation correction by the second-order perturbation method further favors the CTS by 4.7 kcal/mol. Similarly, it entails the reverse tendency that the CTS for butadiene dimerization is more stable than the NTS by a few kcal mol^{-1}. The available experimental results indeed support the CTS.[3f] The hybrid DFT including its correction showed the stabilization of the NTSs with diradical character by the vinyl group. The situation is similar for the cyano group.[3,62]

To confirm the diradical stabilization by phenyl groups, we have carried out the HF, B2LYP, B2′LYP, B3LYP, and BLYP/6-31G* calculations of activation barriers for the Cope rearrangements of phenyl derivatives, assuming the optimized geometries by Hrovat et al.[61] Table 5 summarizes the calculated results. The BS UHF calculations for 2-phenyl and 2,5-diphenyl NTS provide the smaller activation energies than none CTS by about 40−50 kcal mol^{-1} without AP correction. The HF approximation overestimates the diradical stabilization. This tendency remains in the case of B2LYP. On the other hand, the corresponding stabilization for 2,5-diphenyl-1,5-hexadiene is 9.4 kcal mol^{-1} by BLYP, although UBLYP reduces to RBLYP for all of the TSs. It is 8.8 kcal mol^{-1} by B3LYP, slightly smaller than experimental estimation.[63] To understand the diradical stabilization by the phenyl group, HONO and LUNO of 2,5-diphenyl NTS are depicted in Figure 9. From Figure 9, they are delocalized over the phenyl group, showing the conjugation between the allyl radical site and the phenyl group.

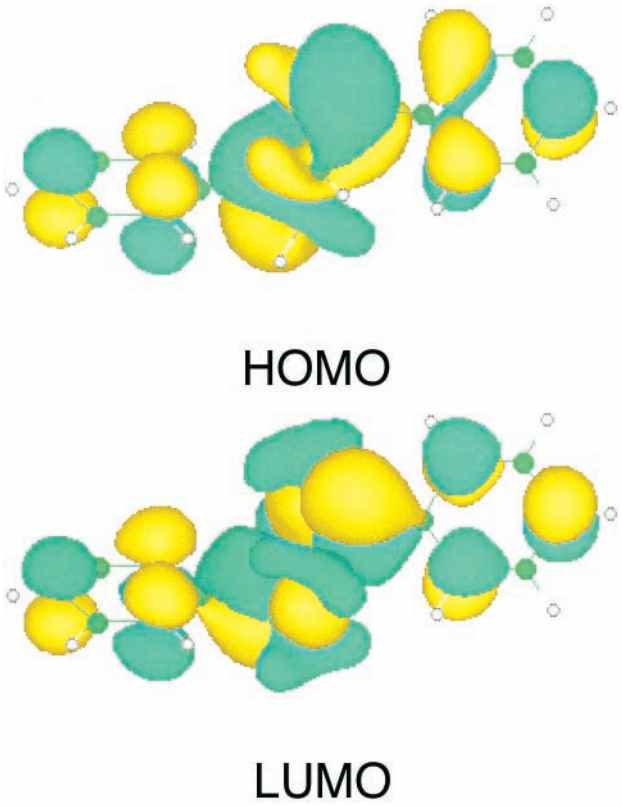

Figure 9. HOMO and LUMO of the NTS for the Cope rearrangement reaction of 2,5-diphenyl-1,5-hexadiene.

The activation enthalpies by B3LYP for 1,5-hexadiene and 2-phenyl-1,5-hexadiene are in excellent agreement with the experimental values,[63] while the slightly large value is given by this method for 2,5-diphenyl-1,5-hexadiene. NO analyses were performed to elucidate the nature of the chemical bonds at the NTSs.[64] The occupation numbers of LUMO for 2-phenyl NTS are 0.688, 0.413, 0.106, and 0.000 by UHF, UB2LYP, UB3LYP, and UBLYP, respectively. While those for 2,5-diphenyl NTS are 0.702, 0.387, 0.017, 0.000, respectively. The reduction of π bond order and magnitude of radical character are not so large for these diradical type TSs, although they are significant for the DIs, as shown in Table S7. It is noticeable that the diradical character by UB3LYP for 2,5-diphenyl NTS collapses into almost zero ($y_{HOMO} = 0.01\%$). This is why UB3LYP calculation is unsuccessful in this system. It was found from Table 5 that UB2′LYP ($C_1 = 40\%$) calculation reproduces the experimental activation enthalpy for 2,5-diphenyl NTS. The hybrid DFT followed by the adjustment of the hybrid parameter C_1 is also effective for the Cope rearrangement reactions.

Stereospecificity of the Diels−Alder Reactions. The B3LYP and BLYP calculations on the Cope rearrangement of two phenyl-substituted 1,5-hexadiene underestimate the diradical

character of NTS, while the UHF and B2LYP overestimate it. The well-balanced description is obtained by the modification of the B2LYP method. This case may be true of the system **IV** for the Diels−Alder reaction, because the I_n value for the CTS increases from 20 (**I**) to 37% (**IV**) by UHF. There is a similar tendency (16 → 37%) for the CTS of the Cope rearrangements involving phenyl substituents at C_2 and C_5 as shown in Table S7. The instability of the chemical bonds for both nonsynchronous CTSs increases gradually when the phenyl group is introduced at the active site.[65] We found from Table S6 that the UB2′LYP ($C_1 = 40\%$) calculation[66] exhibits weak diradical character ($y_{HOMO} = 0.8\%$) at the B3LYP CTS geometry of **IV**, although the UB2′LYP ($C_1 = 30\%$),[66] UB3LYP, and UBLYP solutions reduce to restricted ones. On the analogy of the Cope rearrangement, this small value may be attributed to the diradical stabilization at the highly asymmetric geometry caused by the presence of two phenyl groups in the ortho orientation. The transition from a synchronous CTS to a nonsynchronous NTS with strong diradical character may be gradual, permitting the existence of the intermediate type nonsynchronous TS with moderate diradical character. According to this transition, the flexibility of the system should increase gradually. This weak diradical character, therefore, does not necessarily mean the loss of stereoselectivity for this reaction channel, because the strong π bond ($b^{\pi}_{HOMO} = 0.88$) prevents the rotation around the C_5-C_6 bond, while the ring closure to the cycloproduct through an elusive gauche-in DI seems to be quite probable as illustrated in Figure 5. In this case, this gauche-in nonsynchronous TS is similar to that of a two stage mechanism without a discrete DI,[67] but the location of the gauche-in TS and DI by UB2′LYP is inevitable for more accurate discussion. On the other hand, the anti nonsynchronous TS ($b^{\pi}_{HOMO} = 0.57$) is likely to collapse into flexible, diradicaloid structure such as the anti DI ($b^{\pi}_{HOMO} = 0.12$) as illustrated in Figure 5. The rotational TS[68] around the C_4-C_5 bond from anti to gauche-in conformation also exhibits strong diradical character ($y_{HOMO} = 57\%$) at the UB3LYP level. We must distinguish between nonsynchronous TS with weak diradical character and diradical TS (or DI) with strong diradical character ($y_{HOMO} > 60\%$ or $b^{\pi}_{HOMO} < 0.20$), for which the free rotation is feasible.[54] From the viewpoint of stereospecificity, the former TS is regarded as a nonsynchronous nonradical TS, instead of a diradical TS in the stepwise mechanism. This discrimination seems a key point for deep understanding of the computational results. Apart from steric effect, the chemical indices will provide important information on the stereospecificity for the pericyclic reactions involving radical stabilizing substituents.

Comparison with Experiment. Two mechanisms, concerted and stepwise via either diradical or zwitterionic intermediates, have been proposed for the Diels−Alder reactions on the experimental grounds.[3] Chemical evidence supports the concerted mechanism in many cases, except for specific systems with radical or charge stabilization groups. In fact, the computational results predict that the radical polymerization occurs for phenyl-substituted dienes because the DIs are favorable energetically. Mikhael et al.[69] have reported that competition between the Diels−Alder reaction and the copolymerization occurs in the reactions of alkyl-substituted dienes with electrophilic olefins. The latter reaction has been explained by participation of the gauche NTS and/or DI. The kinetic measurements by Li et al.[70] also supported the radical copolymerization mechanism for s-trans and gauche dienes. Mark[71] investigated the Diels−Alder reactions of hexachlorocyclopentadiene with *trans*-2-butene and dienophiles, which have radical or charge stabilizers such as *trans*-1,2-dichloroethylene, fumaronitrile, *trans*-stilbene, and fumaric acid dimethyl ester. These reactions exhibit the partial loss of stereochemistry of dienophiles except for 2-butene, indicating the existence of diradical or zwitterionic intermediates stabilized by substituents. Available experiments are consistent with radical stabilizations by substituents, in accord with the presented results. On the other hand, the cycloadditions of hexachlorocyclopentadiene and α-methylstyrene with a deuterium label at the β position produce *exo*-phenyl and *endo*-phenyl adducts with complete retention of alkene stereochemistry.[72] These reactions seem to proceed through the Woodward−Katz two stage mechanism,[67] where TS is regarded as a nonsynchronous nonradical TS from the stereochemical standpoint. This indicates the importance of distinction between nonsynchronous TS with moderate diradical character and diradical TS or DI in terms of the chemical indices defined by the occupation numbers of NOs of both BS and SA methods.

Concluding Remarks. Hybrid DFT methods such as B2′LYP and B3LYP followed by the approximate spin correction are reliable and handy for locations of both concerted and nonconcerted TSs and estimations of their energy differences, which are sensitive to substituents introduced. To elucidate the nature of chemical bonds at TSs, chemical indices such as effective bond order, information entropy, diradical character, and unpaired electron density are expressed by the occupation numbers of NOs of the BS hybrid DFT solutions, since they are equally calculated by the SA CAS approaches for comparison (see Table 2 and Table S6). In fact, a comparison between CASSCF and hybrid DFT for parent systems elucidates effective hybrid DFT methods (B3LYP, B2LYP and/or B2′LYP), which are applicable to larger systems with many substituents. The computational results for the Diels−Alder and the Cope rearrangement reactions have indicated that the present procedures are promising for pericyclic reactions in general. Their utility for magnetic transition metal complexes has been demonstrated elsewhere.[73]

Acknowledgment. This work has been supported by a Grant-in-Aid for Scientific Research (Nos. 10149105 and 14204061) from the Ministry of Education, Science, Sports and Culture, Japan. Y.T. was also supported by Research Fellowships of Japan Society for the Promotion of Science for Young Scientists. We thank Dr. Daisuke Yamaki for helpful discussions.

Supporting Information Available: Data are included as follows: the chemical indices for the σ bond of the C−C elongated ethylene (Table S1); the occupation numbers of NOs for the CTS and NTS by UHF and UB3LYP (Tables S2−S4); relative energies for the Diels−Alder reactions of 1-phenylbutadiene and styrene by the B2′LYP methods (Table S5); the occupation numbers and chemical indices for the CTS, anti NTS, and DI of **II**−**IV** by the hybrid UDFT methods (Table S6); the occupation numbers and chemical indices for the CTS, NTS, and DI of the Cope rearrangements of phenyl-substituted 1,5-hexadienes by the hybrid UDFT methods (Table S7); total energies, total angular momentums, and zero point energies (ZPE) for **I**−**IV** (Tables S8, S9); total energies, total angular momentums, and thermal corrections (TC) of the Cope rearrangement of phenyl-substituted 1,5-hexadienes (Table S10); the Cartesian coordinates of all structures reported (Table S11); variations of effective bond order (b), the decrease of bond order ($1 - b$), unpaired electron density (^{LS}U), spin density index (^{LS}Q), information entropy (I), and diradical character (y) for

the σ and π bond with the C−C elongation of ethylene by UHF, UB2LYP, and UBLYP (Figures S1−S6); the optimized geometries of the CTS, anti NTS, and DI of **I**−**III** (Figure S7); the optimized geometries of the DI and rotational TS of **IV** (Figure S8) (PDF). This material is available free of charge via the Internet at http://pubs.acs.org.

References and Notes

(1) Woodward, R. B.; Hoffmann, R. *Angew. Chem., Int. Ed. Engl.* **1969**, *8*, 781.

(2) (a) Houk, K. N.; González, J.; Li, Y. *Acc. Chem. Res.* **1995**, *28*, 81. (b) Borden, W. T.; Loncharich, R. J.; Houk, K. N. *Annu. Rev. Phys. Chem.* **1988**, *108*, 554.

(3) (a) Goldstein, E.; Beno, B.; Houk, K. N. *J. Am. Chem. Soc.* **1996**, *118*, 6036. (b) Wiest, O.; Houk, K. N. *Top. Curr. Chem.* **1996**, *183*, 1. (c) Wiest, O.; Montiel, D. C.; Houk, K. N. *J. Phys. Chem. A* **1997**, *101*, 8378. (d) Houk, K. N.; Li, Y.; Evanseck, J. D. *Angew. Chem., Int. Ed. Engl.* **1992**, *31*, 682. (e) Houk, K. N.; Lin, Y.-T.; Brown, F. K. *J. Am. Chem. Soc.* **1986**, *108*, 554. (f) Li, Y.; Houk, K. N. *J. Am. Chem. Soc.* **1993**, *115*, 7478. (g) Storer, J. W.; Raimondi, L.; Houk, K. N. *J. Am. Chem. Soc.* **1994**, *116*, 9675.

(4) Townshend, R. E.; Ramunni, G.; Segal, G.; Hehre, W. J.; Salem, L. *J. Am. Chem. Soc.* **1976**, *98*, 2190.

(5) (a) Dewar, M. J. S.; Olivella, S.; Stewart, J. J. P. *J. Am. Chem. Soc.* **1986**, *108*, 5771. (b) Dewar, M. J. S.; Pierini, A. *J. Am. Chem. Soc.* **1984**, *106*, 203.

(6) Bernardi, F.; Bottoni, A.; Field, M. J.; Guest, M. F.; Hillier, I. H.; Robb, M. A.; Venturini, A. *J. Am. Chem. Soc.* **1988**, *110*, 3050.

(7) (a) Yamaguchi, K.; Fueno, T.; Fukutome, H. *Chem. Phys. Lett.* **1973**, *22*, 461 (Part I). (b) Yamaguchi, K.; Yoshioka, Y.; Fueno, T. *Chem. Phys. Lett.* **1977**, *46*, 360. (c)Yamaguchi, K.; Yoshioka, Y.; Takatsuka, K.; Fueno, T. *Theor. Chim. Acta* **1978**, *48*, 185 (Part II). (d) Yamaguchi, K.; Takahara, Y.; Fueno, T.; Houk, K. N. *Theor. Chim. Acta* **1988**, *73*, 337 (Part III). (e) Yamanaka, S.; Okumura, M.; Nakano, M.; Yamaguchi, K. *J. Mol. Struct. (THEOCHEM)* **1994**, *310*, 205 (Part IV). (f) Isobe, H.; Soda, T.; Kitagawa, Y.; Takano, Y.; Kawakami, T.; Yoshioka, Y.; Yamaguchi, K. *Int. J. Quantum Chem.* **2001**, *85*, 34 (Part V).

(8) (a) Yamaguchi, K.; Ohta, K.; Yabushita, S.; Fueno, T. *Chem. Phys. Lett.* **1977**, *49*, 555. (b) Yamaguchi, K. *Int. J. Quantum Chem. Symp.* **1980**, *14*, 269.

(9) (a) Wolinski, K.; Pulay, P. *Chem. Phys. Lett.* **1987**, *140*, 255. (b) Wolinski, K.; Pulay, P. *J. Chem. Phys.* **1987**, *90*, 3647.

(10) (a) Roos, B. O.; Linse, P.; Siegbahn, P. E. M.; Blomberg, M. R. A. *Chem. Phys.* **1982**, *66*, 197. (b) Andersson, K.; Malmqvist, P.-A.; Roos, B. O. *J. Chem. Phys.* **1992**, *96*, 1218.

(11) Head-Gordon, H.; Pople, J. A.; Frisch, M. J. *Chem. Phys. Lett.* **1988**, *153*, 503.

(12) Cízek, J. *Adv. Chem. Phys.* **1969**, *14*, 35.

(13) Pople, J. A.; Head-Gordon, M.; Raghavachari, K.; Trucks, G. W. *Chem. Phys. Lett.* **1989**, *164*, 185.

(14) Parr, R. G.; Yang, W. *Density Functional Theory of Atoms and Molecules*; Oxford University Press: Oxford, 1989.

(15) *Density Functional Theory of Many-Fermion Systems*; Trickey, S. B., Ed.; Advanced Quantum Chemistry, Vol. 21; Academic Press: San Diego, 1990.

(16) *Density Functional Methods in Chemistry*; Labanowski, J. K., Andzelm, J. W., Eds.; Springer: New York, 1991.

(17) Kryachko, E. S.; Ludeña, E. V. *Energy Density Functional Theory of Many-Electron Systems*; Understanding Chemical Reactivity, Vol. 4; Kluwer Academic: Dordrecht, 1990.

(18) Pople, J. A.; Gill, P. M. W.; Johnson, B. G. *Chem. Phys. Lett.* **1992**, *199*, 557.

(19) Becke, A. D. *Phys. Rev. A* **1988**, *38*, 3098.

(20) Lee, C.; Yang, W.; Parr, R. G. *Phys. Rev. B* **1988**, *37*, 785.

(21) Becke, A. D. *J. Chem. Phys.* **1993**, *98*, 5648.

(22) (a) Staroverov, V. N.; Davidson, E. R. *J. Am. Chem. Soc.* **2000**, *122*, 186. (b) Staroverov, V. N.; Davidson, E. R. *Chem. Phys. Lett.* **2000**, *330*, 161. (c) Staroverov, V. N.; Davidson, E. R. *J. Am. Chem. Soc.* **2000**, *122*, 7377.

(23) (a) Yamaguchi, K. *Chem. Phys. Lett.* **1975**, *33*, 330. (b) Yamaguchi, K. *Chem. Phys. Lett.* **1979**, *66*, 395. (c) Yamaguchi, K. In *Self-Consistent Field Theory and Applications*; Carbo, R., Klobukowski, M., Eds.; Elsevier: Amsterdam, 1990. (d) Yamaguchi, K.; Okumura, M.; Takada, K.; Yamanaka, S. *Int. J. Quantum Chem.* **1993**, *27*, 201.

(24) Löwdin, P.-O. *Phys. Rev.* **1955**, *97*, 1474.

(25) Takatsuka, K.; Fueno, T.; Yamaguchi, K. *Theor. Chim. Acta* **1978**, *48*, 175.

(26) (a) Shannon, C. E. *Bell. Syst. Technol.* **1948**, *27*, 379. (b) Helstrom, C. W. *Quantum Detection and Estimation Theory*; Academic Press: New York, 1976. (b) Oya, M. *IEEE Trans. Inf. Theory* **1983**, *29*, 70.

(27) Jaynes, E. In *Papers on Probability, Statics and Statistical Physics*; Rosencrantz, R., Ed.; Reidel: Dordrecht, 1993.

(28) Collins, D. M. *Z. Naturforsch.* **1993**, *48A*, 68.

(29) (a) Ramírez, J. C.; Soriano, C.; Esquivel, R. O.; Sagar, R. P.; Hô, M.; Smith, V. H., Jr. *Phys. Rev. A* **1997**, *56*, 4477. (b) Smith, G. T.; Schmider, H. L.; Smith, V. H., Jr. *Phys. Rev. A* **2002**, *65*, 032508.

(30) Fukutome, H. *Prog. Theor. Phys.* **1973**, *47*, 1156.

(31) Cízek, J.; Paldus, J. *J. Chem. Phys.* **1967**, *47*, 4976.

(32) Paldus, J.; Cízek, J. *J. Chem. Phys.* **1970**, *52*, 2919.

(33) Yamaguchi, K. *Chem. Phys. Lett.* **1979**, *68*, 477.

(34) Nishino, M.; Yamanaka, S.; Yoshioka, Y.; Yamaguchi, K. *J. Phys. Chem. A* **1997**, *101*, 705.

(35) Isobe, H.; Takano, Y.; Kitagawa, Y.; Kawakami, T.; Yamanaka, S.; Yamaguchi, K.; Houk, K. N. *Mol. Phys.* **2002**, *100*, 717 (Part VI).

(36) Frisch, M. J.; Trucks, G. W.; Schlegel, H. B.; Gill, P. M. W.; Johnson, B. G.; Robb, M. A.; Cheeseman, J. R.; Keith, T.; Petersson, G. A.; Montgomery, J. A.; Raghavachari, K.; Al-Laham, M. A.; Zakrzewski, V. G.; Ortiz, J. V.; Foresman, J. B.; Cioslowski, J.; Stefanov, B. B.; Nanayakkara, A.; Challacombe, M.; Peng, C. Y.; Ayala, P. Y.; Chen, W.; Wong, M. W.; Andres, J. L.; Replogle, E. S.; Gomperts, R.; Martin, R. L.; Fox, D. J.; Binkley, J. S.; Defrees, D. J.; Baker, J.; Stewart, J. P.; Head-Gordon, M.; Gonzalez, C.; Pople, J. A. *Gaussian 94*, revision E.3; Gaussian, Inc.: Pittsburgh, PA, 1995.

(37) Schmidt, M. W.; Baldridge, K. K.; Boatz, J. A.; Elbert, S. T.; Gordon, M. S.; Jensen, J. J.; Koseki, S.; Matsunaga, N.; Nguyen, K. A.; Su, S.; Windus, T. L.; Dupuis, M.; Montgomery, J. A. *J. Comput. Chem.* **1993**, *14*, 1347.

(38) Petterson, G. A.; Al-Laham, M. A. *J. Chem. Phys.* **1991**, *75*, 1843.

(39) Vosko, S. H.; Wilk, L.; Nusair, M. *Can. J. Phys.* **1980**, *58*, 1200.

(40) Yamaguchi, K.; Takahara, Y.; Fueno, T. In *Applied Quantum Chemistry*; Smith, V. H., Ed.; Reidel: Dordrecht, 1986; p 155.

(41) Yamaguchi, K.; Jensen, F.; Dorigo, A.; Houk, K. N. *Chem. Phys. Lett.* **1988**, *149*, 537.

(42) Soda, T.; Kitagawa, Y.; Onishi, T.; Takano, Y.; Shigeta, Y.; Nagao, H.; Yoshioka, Y.; Yamaguchi, K. *Chem. Phys. Lett.* **2000**, *319*, 223.

(43) (a) Goto, K.; Kubo, T.; Yamamoto, K.; Nakasuji, K.; Sato, K.; Shiomi, D.; Takui, T.; Kubota, M.; Kobayashi, T.; Yakushi, K.; Ouyang, J. *J. Am. Chem. Soc.* **1999**, *121*, 1619. (b) Takano, Y.; Taniguchi, T.; Isobe, H.; Kubo, T.; Morita, Y.; Yamamoto, K.; Nakasuji, K.; Takui, T.; Yamaguchi, K. *J. Am. Chem. Soc.* **2002**, *124*, 11122.

(44) The detailed results are given in the Supporting Information, Table S1.

(45) Diels, O.; Alder, K. *Justus Liebigs Ann. Chem.* **1928**, *460*, 98.

(46) Doering, W. v. E.; Roth, W. R.; Breuckmann, R.; Figge, L.; Lennartz, T.-W.; Fessner, W.-D.; Prinzbach, H. *Chem. Ber.* **1988**, *121*, 1.

(47) Uchiyama, M.; Tomioka, T.; Amano, A. *J. Phys. Chem.* **1964**, *68*, 1878.

(48) Rowley, D.; Steiner, H. *Discuss. Faraday Soc.* **1951**, *10*, 198.

(49) (a) Hirao, K. *Chem. Phys. Lett.* **1992**, *190*, 374. (b) Hirao, K. *Chem. Phys. Lett.* **1992**, *196*, 403.

(50) Carpenter, J. E.; Sosa, C. P. *J. Mol. Struct.* (*THEOCHEM*) **1994**, *311*, 325.

(51) (a) Houk, K. N. *J. Am. Chem. Soc.* **1973**, *95*, 4092. (b) Houk, K. N.; Sims, J.; Watts, C. R.; Lushus, L. J. *J. Am. Chem. Soc.* **1973**, *95*, 7301.

(52) The other optimized geometries are displayed in the Supporting Information, Figures S7 (**I**−**III**) and S8 (**IV**).

(53) (a) Kitagawa, Y.; Soda, T.; Shigeta, Y.; Yamanaka, S.; Yoshioka, Y.; Yamaguchi, K. *Int. J. Quantum Chem.* **2001**, *84*, 592. (b) Kitagawa, Y.; Kawakami, T.; Yamaguchi, K. *Mol. Phys.* **2002**, *100*, 1829.

(54) Single point calculations by UB3LYP showed that the required energies for the 90° rotation around the C_5-C_6 bond of the DI (y_{HOMO} = 58%), gauche-out NTS (y_{HOMO} = 9%), and anti NTS (y_{HOMO} = 7%) are 1.8, 15.9, and 16.5 kcal mol^{-1}, respectively.

(55) The detailed data are shown in the Supporting Information, Tables S2 and S3 by UHF and Table S4 by UB3LYP.

(56) The occupation numbers, I_n, U_n, and Y_n values for **II**−**IV** are given in Table S6.

(57) (a) Valdemoro, C. *Phys. Rev. A* **1992**, *45*, 4462. (b) Goedecker, S.; Umrigar, C. J. *Phys. Rev. Lett.* **1998**, *81*, 866. (c) Cioslowski, J.; Pernal, K. *J. Chem. Phys.* **1999**, *111*, 3396. (d) Yasuda, K. *Phys. Rev. A* **2001**, *63*, 032517.

(58) Miehlic, B.; Stoll, H.; Savin, A. *Mol. Phys.* **1997**, *91*, 527.

(59) (a) Gräfenstein, J.; Cremer, D. *Chem. Phys. Lett.* **2000**, *316*, 569. (b) Gräfenstein, J.; Kraka, E.; Cremer, D. *Chem. Phys. Lett.* **1998**, *288*, 593.

(60) Doering, W. von E.; Birladeanu, L.; Sarma, K.; Blaschke, G.; Scheidemantel, U.; Boese, R.; Benet-Bucholz, J.; Klärner, F.-G.; Gehrke, J.-S.; Zinny, B. U.; Sustmann, R.; Korth, H.-G. *J. Am. Chem. Soc.* **2000**, *122*, 193.

(61) Harovat, D. A.; Chen, J.; Houk, K. N.; Borden, W. T. *J. Am. Chem. Soc.* **2000**, *122*, 7456.

(62) Hrovat, D. A.; Beno, B. R.; Lange, H.; Yoo, H.-Y.; Houk, K. N.; Borden, W. T. *J. Am. Chem. Soc.* **1999**, *121*, 10529.

(63) (a) Dewar, M. J. S.; Wade, L. E. *J. Am. Chem. Soc.* **1977**, *99*, 4417. (b) Doering, W. von E.; Toscano, V. G.; Beasley, G. H. *Tetrahedron* **1971**, *27*, 5299. (c) Roth, W. R.; Lennartz, H.-W.; Doering, W. von E.; Birladeanu, L.; Guyton, C. A.; Kitagawa, T. *J. Am. Chem. Soc.* **1990**, *112*, 1722.

(64) The occupation numbers, I_n, U_n, and Y_n values for the Cope rearrangements are given in Table S7.

(65) The I_n value for the meta CTS of the system **IV** is 30% by UHF. This value is equal to that of **III**.

(66) Relative energies calculated by B2′LYP are shown in Table S5.

(67) Woodward, R. B.; Katz, R. *Tetrahedron* **1959**, *5*, 70.

(68) This saddle point was located 2.6 kcal mol^{-1} above the anti DI and 3.2 kcal mol^{-1} below the anti NTS at the UB3LYP level.

(69) (a) Mikhael, M, G.; Padias, A. B.; Hall, H. K., Jr. *Macromolecules* **1993**, *26*, 5835. (b) Mikhael, M, G.; Padias, A. B.; Hall, H. K., Jr. *Macromolecules* **1994**, *27*, 7339.

(70) Li, Y.; Padias, A. B.; Hall, H. K., Jr. *J. Org. Chem*. **1993**, *58*, 7049.

(71) Mark, V. *J. Org. Chem.* **1974**, *39*, 3179, 3181.

(72) Lambert, J. B.; McLaughlin, C. D.; Mark, V. *Tetrahedron* **1976**, *32*, 2075.

(73) Takano, Y.; Kitagawa, Y.; Onishi, T.; Yoshioka, Y.; Yamaguchi, K.; Koga, N.; Iwamura, H. *J. Am. Chem. Soc.* **2002**, *124*, 450.